



Contents lists available at ScienceDirect

Journal of Quantitative Spectroscopy & Radiative Transfer

journal homepage: www.elsevier.com/locate/jqsrt

First global observations of atmospheric COClF from the Atmospheric Chemistry Experiment mission

Dejian Fu^{a,b,*}, Chris D. Boone^a, Peter F. Bernath^{a,c}, Debra K. Weisenstein^d,
Curtis P. Rinsland^e, Gloria L. Manney^{b,f}, Kaley A. Walker^{a,g}

^a Department of Chemistry, University of Waterloo, Waterloo, Canada ON N2L 3G1

^b NASA Jet Propulsion Laboratory/California Institute of Technology, Pasadena, CA 91101, USA

^c Department of Chemistry, University of York, York YO10 5DD, UK

^d Atmospheric and Environmental Research, Inc., Lexington, MA 02421, USA

^e NASA Langley Research Center, Science Directorate, Hampton, VA 23681, USA

^f Department of Physics, New Mexico Institute of Mining and Technology, Socorro, NM 87801, USA

^g Department of Physics, University of Toronto, Toronto, Canada ON M5S 1A7

ARTICLE INFO

Article history:

Received 3 September 2008

Received in revised form

17 February 2009

Accepted 18 February 2009

Keywords:

Remote sensing

Stratospheric chemistry

Infrared atmospheric remote sounding

Measurement-model comparisons

Stratospheric chlorine chemistry

Stratospheric fluorine chemistry

COClF

CCl₃F

ABSTRACT

Carbonyl chlorofluoride (COClF) is an important reservoir of chlorine and fluorine in the Earth's atmosphere. Satellite-based remote sensing measurements of COClF, obtained by the Atmospheric Chemistry Experiment (ACE) for a time period spanning February 2004 through April 2007, have been used in a global distribution study. There is a strong source region for COClF in the tropical stratosphere near 27 km. A layer of enhanced COClF spans the low- to mid-stratosphere over all latitudes, with volume mixing ratios of 40–100 parts per trillion by volume, largest in the tropics and decreasing toward the poles. The COClF volume mixing ratio profiles are nearly zonally symmetric, but they exhibit a small hemispheric asymmetry that likely arises from a hemispheric asymmetry in the parent molecule CCl₃F. Comparisons are made with a set of in situ stratospheric measurements from the mid-1980s and with predictions from a 2-D model.

© 2009 Elsevier Ltd. All rights reserved.

1. Introduction

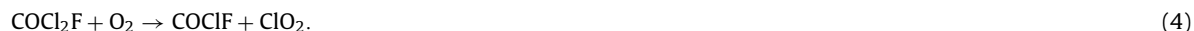
Carbonyl chlorofluoride (COClF) is a reservoir species for both fluorine and chlorine [1–6]. In the tropics, COClF was predicted to make the largest contribution (about 50%) to the total amount of inorganic fluorine ($F_y = HF + COF_2 + COClF$) in the altitude range of about 17–26 km [6]. Fluorine is not directly involved in the chemical reactions that destroy ozone. The primary interest in monitoring F_y is as a surrogate for its precursors (mainly the long-lived chlorofluorocarbons (CFCs) and hydrochlorofluorocarbons (HCFCs)) that have been photodissociated.

Although CFC-12 (difluorodichloromethane, CCl₂F₂) is the most abundant fluorine-containing source gas, and therefore appears to be a good candidate as a source for COClF, CFC-12 most likely breaks down to form COF₂ instead of COClF [6,7]. The major source of atmospheric COClF is decomposition of CFC-11 (trichlorofluoromethane, CCl₃F). The reason for this is that the C–Cl bonds break more readily than C–F bonds for CFCs due to the smaller bond energy of a C–Cl bond. Production of COClF is expected to occur mostly above the troposphere, where significant photodissociation of CFC-11 can occur. The currently accepted mechanism for stratospheric photo-oxidation reactions of CFC-11 is

* Corresponding author at: Department of Chemistry, University of Waterloo, Waterloo, Canada ON N2L 3G1.

E-mail address: dfu@scisat.ca (D. Fu).

as follows:



COCIF can be removed by photodissociation at high altitudes or through reaction with oxygen atoms. The corresponding pathways are as follows:



COCIF has been studied using both models and experiments. Sze [8] and Crutzen et al. [9] examined vertical distributions of the fluorine containing reservoir species HF, CF₂O, and COCIF for 1976 and 1977, respectively, using a one-dimensional (1-D) model. Wilson et al. [10] measured concentrations of COCIF in the upper troposphere and lower stratosphere during five northern middle latitude aircraft flights (50°N–78°N) in 1986 and 1987, using the matrix isolation–Fourier transform infrared spectroscopy technique. Kaye et al. [6] investigated the vertical, meridional, and seasonal dependence of HF, COF₂, and COCIF for the year 1989 using a two-dimensional (2-D) model.

Rinsland et al. [11] reported the first remote sensing retrievals of COCIF using solar occultation measurements from Fourier transform spectrometer on the Atmospheric Chemistry Experiment (ACE) mission [12,13], with an analysis approach that employed spectra averaged over many different occultations. Spectroscopic parameters for COCIF were lines taken from the 1995 Atmospheric Trace Molecule Spectroscopy (ATMOS) Experiment (ATMOS) supplemental linelist [14,15]. Rinsland et al. focused on measurements in the latitude regions of tropical–subtropical (20°S–20°N) and northern mid-latitudes (30–50°N). In addition, the results were compared with predictions from the Atmospheric and Environmental Research (AER), Inc. 2-D model. Significant differences were observed between the measured altitude peaks of the COCIF volume mixing ratio (VMR) profiles and those predicted by the AER model.

This paper investigates reasons for the disagreement in the previous work between measured COCIF and AER model results. It also provides the first global distribution study for the molecule.

2. Measurements from ACE mission

ACE is a Canadian-led satellite mission for remote sensing of the Earth's atmosphere from a low Earth circular orbit (altitude 650 km, inclination 74°). The ACE satellite, also known as SCISAT-1, was launched on 12 August 2003 and began science operations in February 2004. The primary instrument on SCISAT-1 is a Fourier transform spectrometer called the ACE-FTS, featuring a high spectral resolution of 0.02 cm⁻¹ (±25 cm maximum optical path difference) and broad spectral coverage in the mid-IR: 750–4400 cm⁻¹ [12]. The ACE-FTS records spectra by solar occultation in which the sun is used as a light source and spectra are recorded in the limb geometry during sunrise and sunset. The measurements are used to obtain VMR profiles for trace gases in the Earth's atmosphere, along with pressure and temperature profiles, with a vertical resolution of 3–4 km [13]. The current processing version for the ACE-FTS is version 2.2, with updates for O₃, N₂O₅, and HDO.

COCIF VMR retrievals were performed using selected microwindows in the ν₁ band (~1876 cm⁻¹) region of COCIF. The eight microwindows used for the retrievals are reported in Table 1, along with the interfering species that were retrieved simultaneously. The microwindow near 1882 cm⁻¹ contains a minor interference due to OCS, with less than 1% absorption at the lowest altitudes in the tropics (and a decreasing contribution at higher altitudes and different latitudes). This interference is not retrieved simultaneously, but its contribution to the spectrum is known sufficiently accurately from the ACE-FTS version 2.2 retrieval results. The altitude ranges for the microwindows vary as a function of latitude. The form of the latitudinal variation was chosen to make use of as much of the COCIF information in the measurements as possible without “fitting noise” (i.e., analyzing spectra for which the contribution from COCIF was below the instrument noise level). In the spectral region containing the microwindows, water vapor strongly saturates in the upper troposphere/lower stratosphere, making it impossible to extend the retrievals below ~13 km. This is not a major concern, since the concentration of COCIF in the troposphere is minimal, for example typically less than 4 parts per trillion by volume (pptv) in observations made by Wilson et al. [10] in the 1980s.

COCIF spectroscopic parameters were taken from the ATMOS supplemental list [14,15]. The spectroscopic data reported for the molecule is described as being very crude, with a factor of three uncertainty in intensities. Every line in the spectrum is also assigned a single value for the lower state energy, a single common air broadening coefficient, and a common temperature dependence for the air broadening coefficient. Line parameters for all other molecules were taken from the HITRAN 2004 database [16]. Pressure and temperature for the retrievals were taken from ACE-FTS version 2.2 results.

Table 1

Spectral range, altitude range, and interfering species used in the retrievals of COCIF volume mixing ratios.

Spectral range of microwindows ^a (cm ⁻¹)	Altitude range ^b (km)				Interfering species ^c
	0°	30°N or 30°S	60°N or 60°S	90°N or 90°S	
1862.100–1863.100					H ₂ O, CO ₂ , O ₃ , NO, N ₂ O, H ₂ ¹⁷ O, ¹⁶ O ¹³ C ¹⁶ O, ¹⁶ O ¹² C ¹⁸ O
1864.100–1864.700					
1864.975–1865.825					
1866.645–1866.995					
1867.230–1867.530	15.0–32.0	14.7–31.1	13.7–27.3	13.0–24.2	
1869.805–1870.155					
1870.350–1870.650					
1881.300–1882.000					

^a Microwindows were selected from the COCIF ν_1 fundamental band ($\nu_0 = 1876 \text{ cm}^{-1}$) spanning the 1790–1910 cm^{-1} range.

^b Altitude range was set in the retrievals by using the equations Bottom Layer Altitude = $15 - 2 \times |\sin(\text{latitude of tangent point})|^{3/2}$ and top layer altitude = $32 - 6.8 \times |\sin(\text{latitude of tangent point})|^{3/2} - |\sin(\text{latitude of tangent point})|^{9/2}$. The altitude ranges of four representative latitudes were shown for the southern hemisphere and the northern hemisphere.

^c Interfering species were fitted simultaneously with COCIF in all microwindows. The altitude range for the interfering species is the same as that of COCIF except for ¹⁶O¹²C¹⁶O, which is only used below 21 km at all latitudes.

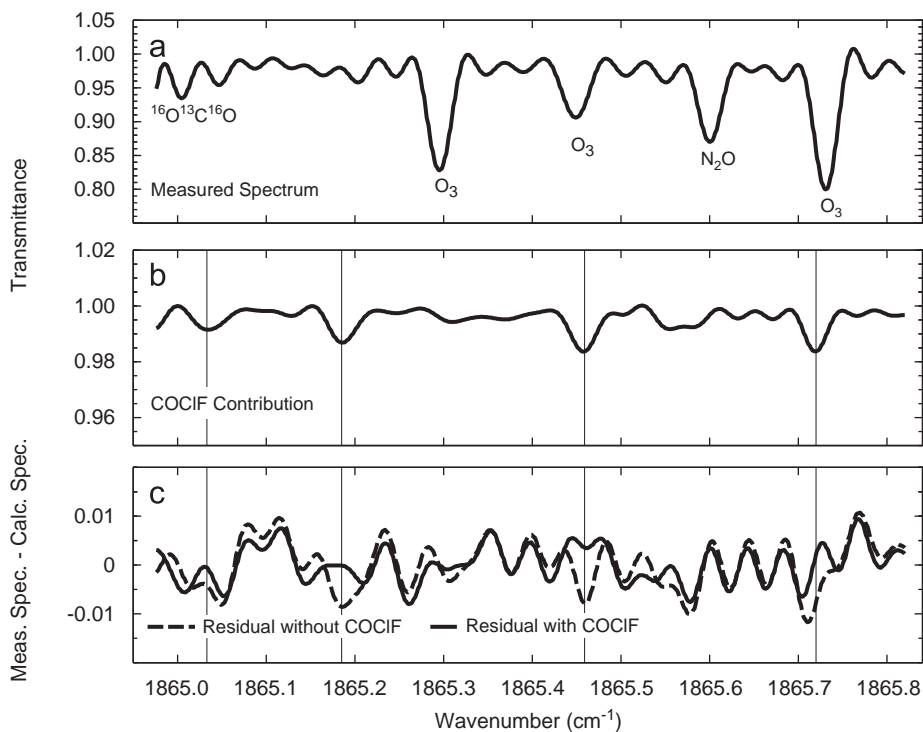


Fig. 1. Spectral region 1864.975–1865.825 cm^{-1} used in the retrieval of COCIF VMR for this study is displayed: (a) a spectrum observed at 24.2 km in the tropics (latitude 3.82°S; longitude 33.93°E) on 23 August, 2005; (b) the COCIF contribution to the spectrum; (c) present the residuals (measured spectrum–calculated spectrum) when COCIF is excluded (dashed lines) or included in the calculation (solid lines), respectively. Vertical solid lines in (b) and (c) show the centers of COCIF absorption lines.

Fig. 1 shows an example of the residuals observed for a particular microwindow, both with and without COCIF included in the calculated spectrum. The example uses a single measurement near 24.2 km in a tropical occultation (latitude 3.82°S; longitude 33.93°E) collected on 23 August 2005. The microwindow (1864.975–1865.825 cm^{-1}) is located near the maximum of COCIF absorption in the P branch. Vertical solid lines in panels b and c of Fig. 1 show the centers of COCIF absorption lines and illustrate where to look for the largest changes in the residuals. The contribution of COCIF to the spectrum is very weak, the order of 1–2%, but the evidence that the spectral features belong to COCIF is conclusive. It is worth noting that fitting residuals in the COCIF microwindows generally have a systematic component, likely from limits in

spectroscopic knowledge for the region. These systematic components are larger than residuals due to random noise (the signal-to-noise ratio for the ACE-FTS in this spectral region is about 340:1) and are not reduced in magnitude by averaging multiple occultations. Thus, the residuals from a single measurement are comparable to the residuals shown in the paper by Rinsland et al. [11] for averaged occultations.

Systematic errors in the retrieval of COCIF VMR mainly arise from the crude spectroscopic parameters of COCIF [11]. Random errors (e.g., from measurement noise and deficiencies in the retrievals of interfering species) are taken as the statistical fitting errors from the nonlinear least squares process (i.e., the square root of the diagonal elements of the covariance matrix). Near the peak of the COCIF VMR profile, the random error was about 20% of the retrieved value. Near the top of the altitude range, where the VMR values were small and the COCIF signal approached the noise level, random errors often exceeded 100%. Random errors are greatly reduced by working with average profiles rather than a single profile. For VMR profiles presented in this article, random contributions to the uncertainty are generally less than 4 pptv because of the use of average profiles.

A large volume of air within the polar vortex experiences a significant subsidence during the polar winter and spring seasons. Consequently, VMR profiles of COCIF measured inside or at the edge of the polar vortex will peak at lower altitudes than profiles measured outside the vortex. To eliminate the contribution of this temporary dynamical effect from the observed global distribution of COCIF VMRs, measurements carried out inside the polar vortex or on the vortex edge were excluded from analysis. Using potential vorticity (PV) at the ACE measurement locations from the Met Office Derived Meteorological Products (DMPs) described by Manney et al. [17] in 2007, a two-step approach similar to that described by Nassar et al. [18] and Fu et al. [19] was used to classify each of the 10783 occultations collected during the period February 2004–April 2007 into three categories: inside, outside, or on the edge of the vortex. Those occultations recorded inside or on the edge of the vortex were filtered out, and the remaining 8368 extravortex occultations were then used in the evaluation of the COCIF global distribution. The locations of these 8368 occultations have an even distribution in general and provided global coverage. As a solar occultation mission, the geographic coverage from ACE is relatively sparse, collecting just 30 occultations per day. However, over the course of several years, a degree of global coverage is achieved, with the highest density of measurements toward the poles, a consequence of the high inclination orbit (74°).

3. Measurements from ATMOS experiment

The ATMOS experiment was designed to study the chemical composition of the atmosphere from space, and was carried for four flights on the Space Shuttle in the 1980s and 1990s [20]. The ATMOS instrument is a Fourier transform spectrometer that recorded spectra containing COCIF absorption features in the solar occultation viewing geometry in three spectral regions: filter 2 (1100–2000 cm⁻¹), filter 3 (1580–3400 cm⁻¹), and filter 9 (600–2450 cm⁻¹). With these data, we can look at historical “snapshots” of COCIF VMRs in particular latitude bands. The signal-to-noise ratio of ATMOS spectra in the COCIF MWs listed in Table 1 (about 170:1, 75:1, and 120:1 for filters 2, 3, and 9, respectively) is generally lower than that of ACE-FTS spectra (340:1). In addition, the COCIF signal in the filter 3 region is generally at or below the noise level. Therefore, the ATMOS filter 2 and 9 measurements are more suitable for the retrievals of COCIF VMRs than those of filter 3. Sunset occultations using the ATMOS instrument on Spacelab-3 and ATLAS-1 (Atmospheric Laboratory for Applications and Science) were used to obtain the atmospheric COCIF distribution in 1985 and 1992. The longitude, latitude, date, time and filters of the occultations used are reported in Table 2. The same approach used for the ACE data was applied to the retrieval of COCIF VMRs for the Spacelab-3 and ATLAS-1 spectra. Retrievals were also performed for the other two ATMOS missions (ATLAS-2 and ATLAS-3), but these results are not reported here.

Table 2

Longitude, latitude, date, time, and filters of sunset occultations for the ATMOS instrument on Spacelab-3 and ATLAS-1 (ATmospheric Laboratory for Applications and Science-1).

Space mission	Occultation	Longitude	Latitude	Date (yyyy/mm/dd)	Universal time (hh:mm:ss)	Filter number
Spacelab-3	sl3ss03	69.1°E	31.4°N	1985/04/30	13:58:05	2 ^a
	sl3ss07	91.9°W	29.5°N	1985/05/01	00:39:29	2
	sl3ss12	54.0°W	25.2°N	1985/05/01	22:02:25	2
ATLAS-1	at1ss08	9.9°E	34.0°S	1992/03/26	17:19:00	9 ^b
	at1ss11	58.0°W	34.2°S	1992/03/26	21:50:16	9
	at1ss21	4.4°E	43.8°S	1992/03/28	17:34:32	9
	at1ss29	21.1°W	48.7°S	1992/03/29	19:12:17	9
	at1ss32	89.0°W	48.6°S	1992/03/29	23:43:17	9

^a Filter 2 covers the 1100–2000 cm⁻¹ spectral region.

^b Filter 9 covers the 600–2450 cm⁻¹ spectral region.

4. Prediction from AER 2-D model

Most global chemical transport models do not include COCIF, and the standard AER 2-D chemical transport model [21–23] is no exception. This model has a horizontal resolution of 9.5° from pole to pole. The vertical coordinate is $\log(\text{pressure})$ and provides a vertical resolution of approximately 1.2 km from the surface to 60 km. Model temperatures and transport/circulation are prescribed according to climatology and do not respond to changes in aerosols or chemical species. A special AER model version was created to include COCIF photolysis and the reaction rate between O^1D and COCIF. It was used in the calculations for the global distribution of COCIF VMRs and the results were compared to the ACE measurements. The VMR of CCl_3F , the source of COCIF, was set to 253.26 pptv [24] at the surface boundary to simulate 2004 conditions. The AER model assumes COCIF is immediately produced when CCl_3F reacts. The reaction rates of photolysis and reaction with O^1D were taken from the JPL-2006 data to calculate the loss of COCIF [25] in the stratosphere. From surface up to 10 km, the AER model assumes COCIF loss by washout that has a first-order life time against washout set as 5 days at 0–2 km, increasing to 40 days at 8.8–10 km. The VMRs of COCIF for the middle of each month were output from the model and interpolated from pressure grid to geometric altitude with a uniform layer thickness of 1 km. The change of COCIF VMRs in the AER model prediction over the time period spanned by this study is expected to be minor because the boundary condition for CCl_3F will not change more than 4% from 2004 to 2007. Therefore, in this work, the global distribution of COCIF predicted by the AER model using the CCl_3F boundary condition from 2004 was compared to the entire set of ACE-FTS measurements between February 2004 and April 2007.

5. Results and discussion

Within 5-degree latitudinal zones, the observed VMR profiles of COCIF show very similar characteristics in terms of peak altitude and VMR values at the peak. The entire data set was therefore separated into 5-degree latitude bins for each season from 2004 to 2007 in order to investigate seasonal variations. All of the profiles within a given bin were averaged to

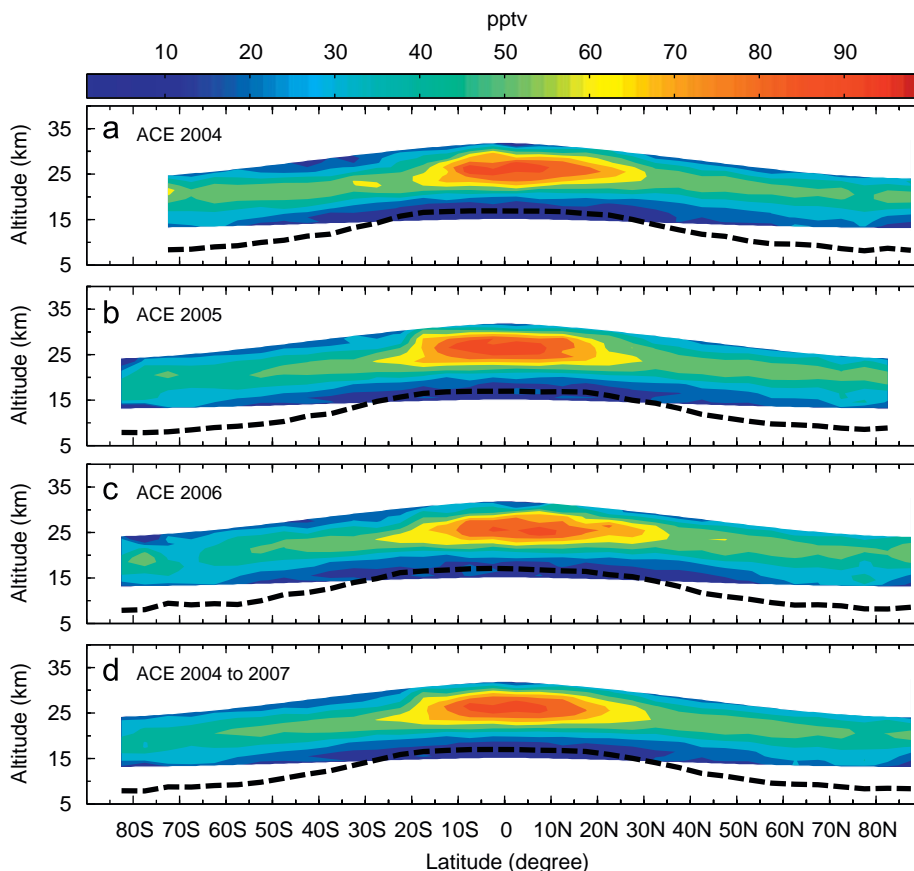


Fig. 2. Latitudinal distributions of annual averaged COCIF VMR profiles (in units of pptv) from the ACE-FTS observations in (a) 2004; (b) 2005; (c) 2006; and of averaged for entire data set (d) February 2004–April 2007. The black dash line is the average tropopause height from the Met Office model.

generate a single profile with reduced noise. Although there are 36 bins between 90°N and 90°S, only 35 of the bins were populated because there were no profiles in the region 85–90°S. Hence, 35 averaged COCIF VMR profiles for each season were used to generate contour plots (not shown). Similar plots were drawn using the monthly mean VMR profiles from the AER model. We found that seasonal cycles are small in both the ACE-FTS observations and AER predictions and therefore yearly averages were used. Fig. 2 shows contour plots for the measured data, separated by year for 2004, 2005, and 2006, and then averaged over all data (2004–2007). The different plots look very similar, suggesting that interannual variation of COCIF VMR is relatively weak.

Fig. 3 provides a comparison of the ACE-FTS COCIF results (averaged over all measurements) with the AER model results. The agreement is very good. In the lower stratosphere, COCIF has a layer of enhanced VMR (40–100 pptv) with a thickness of 5 to 10 km. Within this layer, COCIF values are highest near the equator and decline poleward. There is a core of strongly enhanced COCIF (VMRs 60–100 pptv) between about 22 and 29 km in the region 20°N–20°S. For all latitudes, the retrieved VMR drops rapidly to zero for altitudes above the COCIF enhancement layer. ACE-FTS measurements of COCIF do not extend into the lower troposphere, because H₂O saturates the spectral region at low altitudes. Where measurements extend into the upper troposphere (such as in the tropics), VMR values are low, in agreement with the model.

The long lifetime of CCl₃F in the troposphere allows it reach the stratosphere following release at the surface. It enters the stratosphere largely through upward motion in the tropics. Chlorine and fluorine atoms are removed from the molecule (preferentially chlorine due to its weaker bond) through photodissociation. In the lower stratosphere, the photodissociation is weak because of shielding of UV radiation by ozone, and so the creation of COCIF is relatively weak in this region. At higher altitudes in the stratosphere, with less shielding, production of COCIF will increase due to increased photolysis. Based on the distribution in Fig. 3, the bulk of atmospheric COCIF appears to be created over the tropics, in large part because the parent molecule, CCl₃F, has the largest stratospheric abundance in the tropics, as will be discussed in more detail later. In addition, there may be a contribution from the fact that the tropics feature greater insolation than higher latitudes due to a smaller solar zenith angle. The lifetime of COCIF in the stratosphere is about 1.62 years and is sufficient for at least some of the COCIF generated in the tropics to be transported poleward by the Brewer–Dobson circulation, adding to the in situ COCIF production occurring at higher latitudes. This is consistent with the high VMR values over the tropics, the decreasing VMR values poleward, and the nearly zonally symmetric pattern centered on the equator. Removal of COCIF is primarily by washout in the troposphere, and by photolysis or reaction with O(¹D) in the stratosphere.

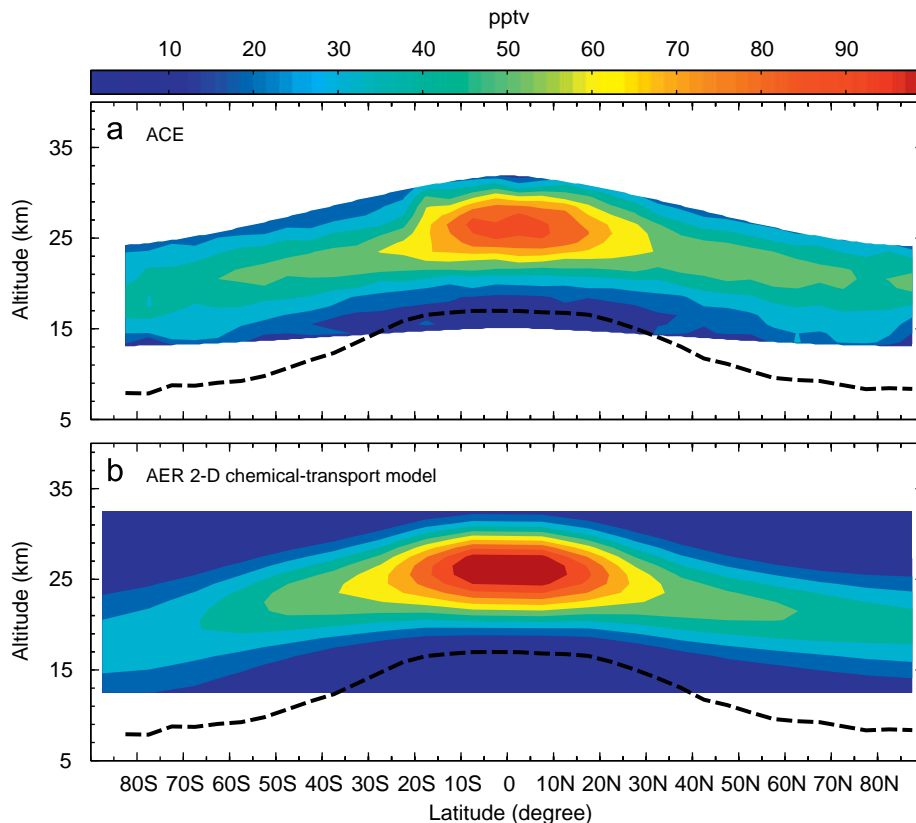


Fig. 3. Comparison of latitudinal distributions of averaged COCIF VMR profiles (in units of pptv) from (a) the ACE-FTS observations during the period February 2004–April 2007; and (b) the AER model prediction are displayed. The black dash line is the average tropopause height from the Met Office model.

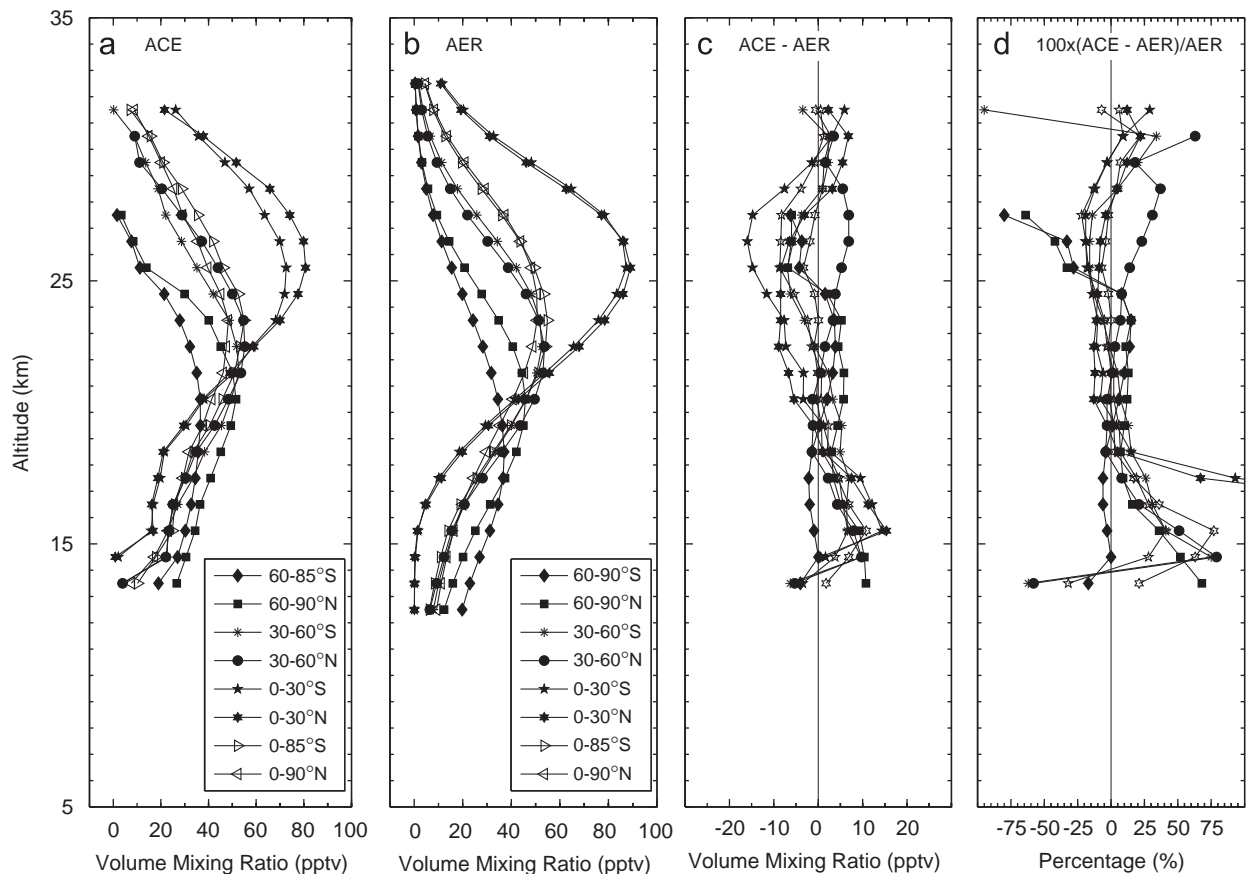


Fig. 4. The averaged COCIF VMR profiles (in units of pptv) for 90–60°N, 60–30°N, 0°N–30°N, 0°S–30°S, 30–60°S and 60–85°S latitudinal zones, and the COCIF VMR profiles for the southern and northern hemispheres: (a) observed by the ACE mission during the period February 2004–April 2007; (b) predicted by the AER model; (c) the differences of averaged COCIF VMR profiles between ACE measurement and the AER model; (d) the percentage differences of averaged COCIF VMR profiles between ACE measurement and the AER model.

Fig. 4(a) shows COCIF profiles corresponding to six different latitudinal zones (90–60°N, 60–30°N, 0°N–30°N, 0°S–30°S, 30–60°S and 60–85°S) together with the southern and northern hemisphere, averaged from observed profiles spanning February 2004 through April 2007. In the stratosphere, the peak values of COCIF VMRs decrease significantly from the tropics to the poles. There is also a small asymmetry with the northern hemisphere having slightly enhanced VMRs relative to the southern hemisphere. The hemispheric differences of COCIF VMRs are generally 10–15 pptv in the measurement altitude range and are significantly larger than the estimated measurement uncertainties (4 pptv). The hemispheric difference has a significant latitudinal dependence. These features are consistent with AER model predictions, as seen in Figs. 3(b) and 4(b). The VMR differences between ACE measurements and model predictions (Fig. 4(c), ACE–AER) are within –7~11 pptv, –5~10 pptv, –9~15 pptv and –16~14 pptv, –7~10 pptv, –6~4 pptv, –9~7 pptv and –3~11 pptv for 90–60°N, 60–30°N, 0°N–30°N, 0°S–30°S, 30–60°S, 60–85°S, 0–90°N and 0–85°S, respectively. The percentage differences between the model predictions and measurements (Fig. 4(d), $100 \times (\text{ACE} - \text{AER}) / \text{AER}$) are about $\pm 10\%$, although the percentage differences tend to be large (about 50%) near the upper and lower altitude limits because of the small COCIF VMR values at these altitudes.

CCl_3F , the source species of COCIF, has been measured by thermal infrared nadir sounders [26,27], limb emission instruments [28,29], and solar occultation sounders [30]. Averaged VMR profiles for CCl_3F from ACE-FTS observations, corresponding to six different latitudinal zones (90–60°N, 60–30°N, 0°N–30°N, 0°S–30°S, 30–60°S and 60–85°S) and the global latitudinal distribution, are shown in Figs. 5 and 6, respectively. These data employ the same set of occultations used in the COCIF analysis, ranging from February 2004–April 2007. In the upper troposphere/lower stratosphere altitude range, CCl_3F VMR decreases significantly from the tropics to the poles. As mentioned previously, the larger amounts of CCl_3F in the tropics contribute to enhanced production of COCIF in that region.

Fig. 5 also shows that CCl_3F VMRs in the northern hemisphere are higher than in the southern hemisphere. Average CCl_3F results for the two hemispheres differ by a roughly constant amount as a function of altitude, about 20 pptv, but there is a significant latitudinal dependence to the difference, as seen in Fig. 5(a). The hemispheric differences in the parent

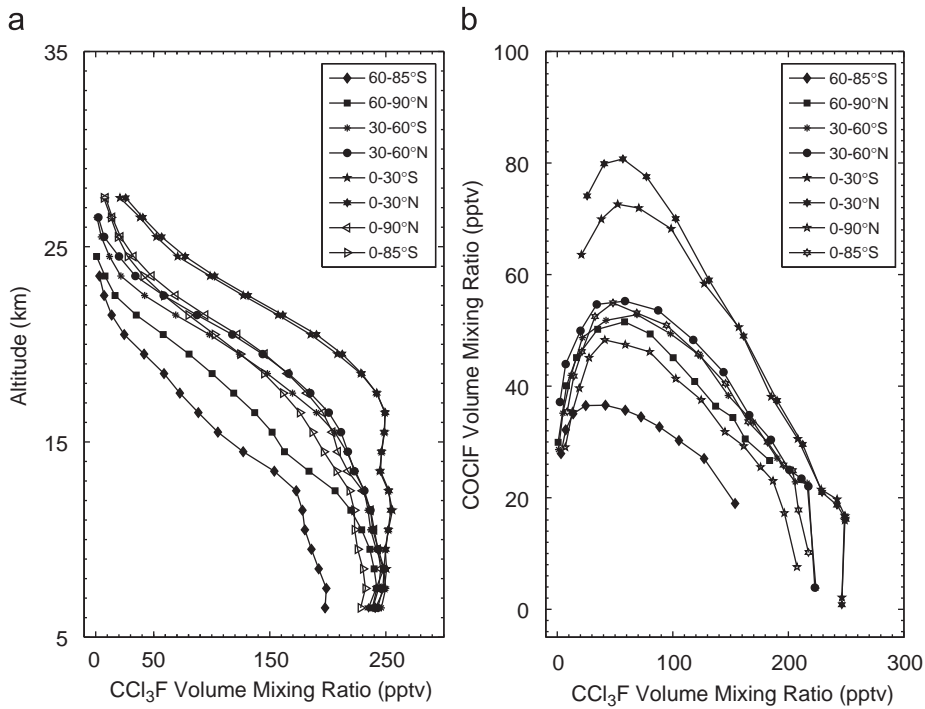


Fig. 5. The averaged CCl_3F VMR profiles (in units of pptv) for (a) 90–60°N, 60–30°N, 0°N–30°N, 0°S–30°S, 30–60°S and 60–85°S latitudinal zones, together with the southern and northern hemisphere and (b) COClF VMR as a function of CCl_3F VMR observed by the ACE mission during the period February 2004–April 2007.

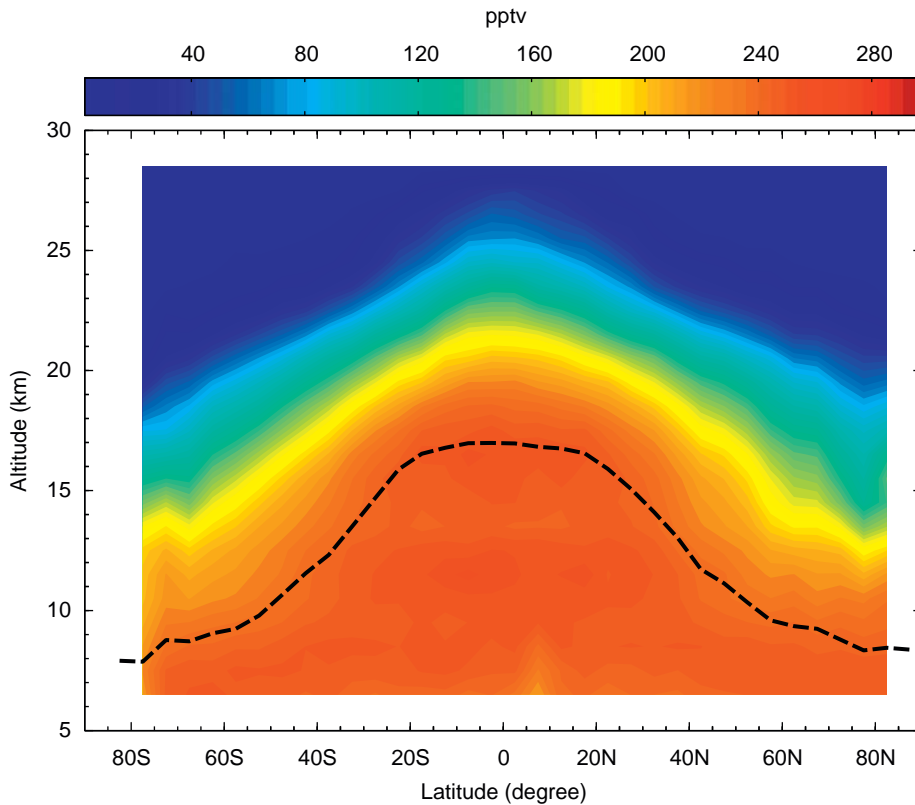


Fig. 6. Latitudinal distributions of averaged CCl_3F VMR profiles (in units of pptv) from the ACE-FTS observations during the period February 2004–April 2007. The black dash line is the average tropopause height from the Met Office model.

molecule CCl_3F explain the slight hemispheric asymmetry in the COCIF data and its latitudinal dependence. This feature is shown clearly in Fig. 5(b) that presents the correlation between CCl_3F VMR and COCIF VMR. Ground-based studies provide further evidence for the hemispheric difference for CCl_3F in the past 30 years, although the amount of CCl_3F and its hemispheric difference have been decreasing over the past 15 years as a result of emission restrictions on CFCs required by the Montreal Protocol and its amendments. For example, the Atmospheric Lifetime Experiment, the Global Atmospheric Gases Experiment and the Advanced Global Atmospheric Gases Experiment (ALE/GAGE/AGAGE) [24,31], the National Oceanic and Atmospheric Administration Climate Monitoring and Diagnostics Laboratory (NOAA/CMDL) [24,32,33], and the University of California at Irvine (UCI) [24,34,35] have measured the surface concentrations of CCl_3F since 1978. Given the 45 year lifetime of CCl_3F , persistence of the hemispheric difference indicates that significant anthropogenic emission is still occurring in the northern hemisphere.

Prior to the ACE mission, only one set of measurements was reported for COCIF VMRs. These measurements were carried out from five Lear Jet flights between Germany and Spitzbergen ($50^\circ\text{--}78^\circ\text{N}$) on 4 December 1986, 1 January 1987, 21 February 1987, 22 April 1987 and 11 June 1987. The VMRs of COCIF were found to be below the detection limit of 4 pptv for altitudes below the tropopause height: 12.1, 9.9, 7.3, 9.5, and 9.4 km for each flight, respectively, determined by averaging radiosonde data. Above the tropopause, COCIF VMRs increased rapidly to 185 pptv at 5 km above the tropopause. However, these aircraft measurements are mainly below the lowest altitude limit of the ACE-FTS retrievals, limiting the usefulness of comparisons. Also, differences are expected due to changes in the parent molecule CCl_3F in the interim. However, it is perhaps worth noting that the general behavior of the VMR vertical structure of COCIF observations in the altitude overlap range (13–17 km) is consistent between the two data sets.

In the previous work on COCIF from ACE-FTS measurements (Rinsland et al. [11]), retrievals were performed on spectra generated by averaging measurements from hundreds of occultations. For the two latitude bands used in that study, comparisons were made with the AER model predictions. Discrepancies were observed between the observed and predicted peak altitude for the COCIF VMR profile, with altitude offsets of 2.5 and 4.5 km for the tropics and northern mid-latitudes, respectively. However, as seen in Fig. 7, no altitude offsets are evident for the retrievals used in the current work. The measured and predicted peak altitudes in the COCIF VMR profile are both around 26.5 km, and the shapes agree quite well. Similarly, the average COCIF VMR profile for northern mid-latitudes ($30^\circ\text{--}50^\circ\text{N}$) from this work peaks near 22.5 km, in agreement with the AER model prediction.

The results from Rinsland et al. employ the same data used in this work. The discrepancies in peak altitude shown in Fig. 7 must therefore arise from differences in the analysis approach. In particular, the current work performs retrievals on individual occultations and then averages the profiles, whereas the previous work averaged the measurements from different occultations (to improve signal-to-noise) and then performed a single retrieval on the set of average spectra. Average spectra were generated from all measurements within a particular altitude “bin”. If the altitude distribution is

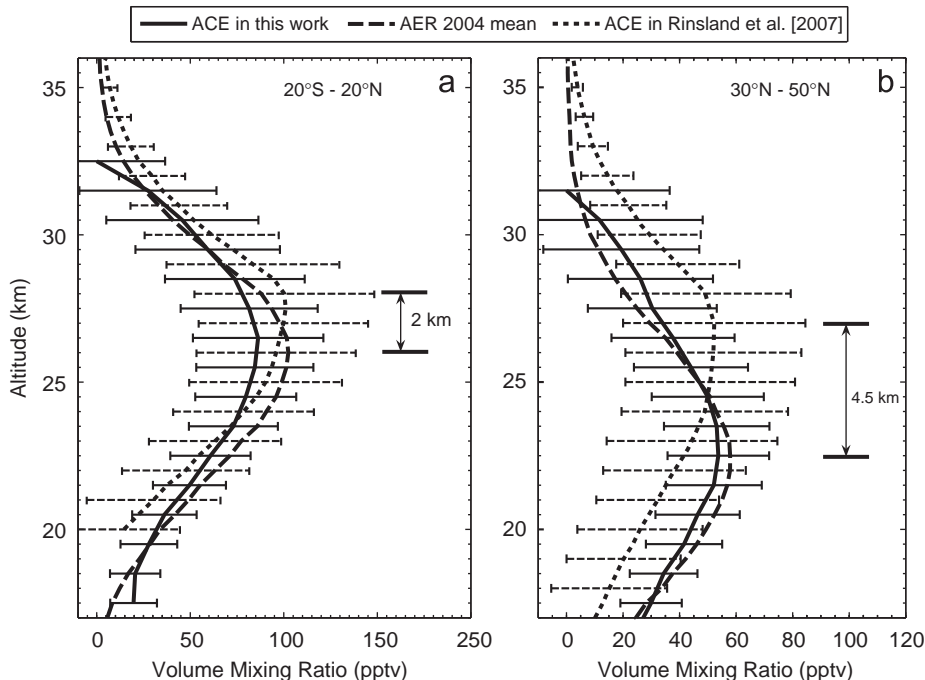


Fig. 7. Comparison of averaged COCIF VMR as function of altitude for (a) tropical latitudes ($20^\circ\text{S}\text{--}20^\circ\text{N}$) and (b) northern mid-latitudes ($30^\circ\text{--}50^\circ\text{N}$) from 2004 and 2005 with AER 2-D model prediction for 2004 (annual average). Error bars are the standard deviation of averaged COCIF VMR profiles and represent a measure of the scatter in the data.

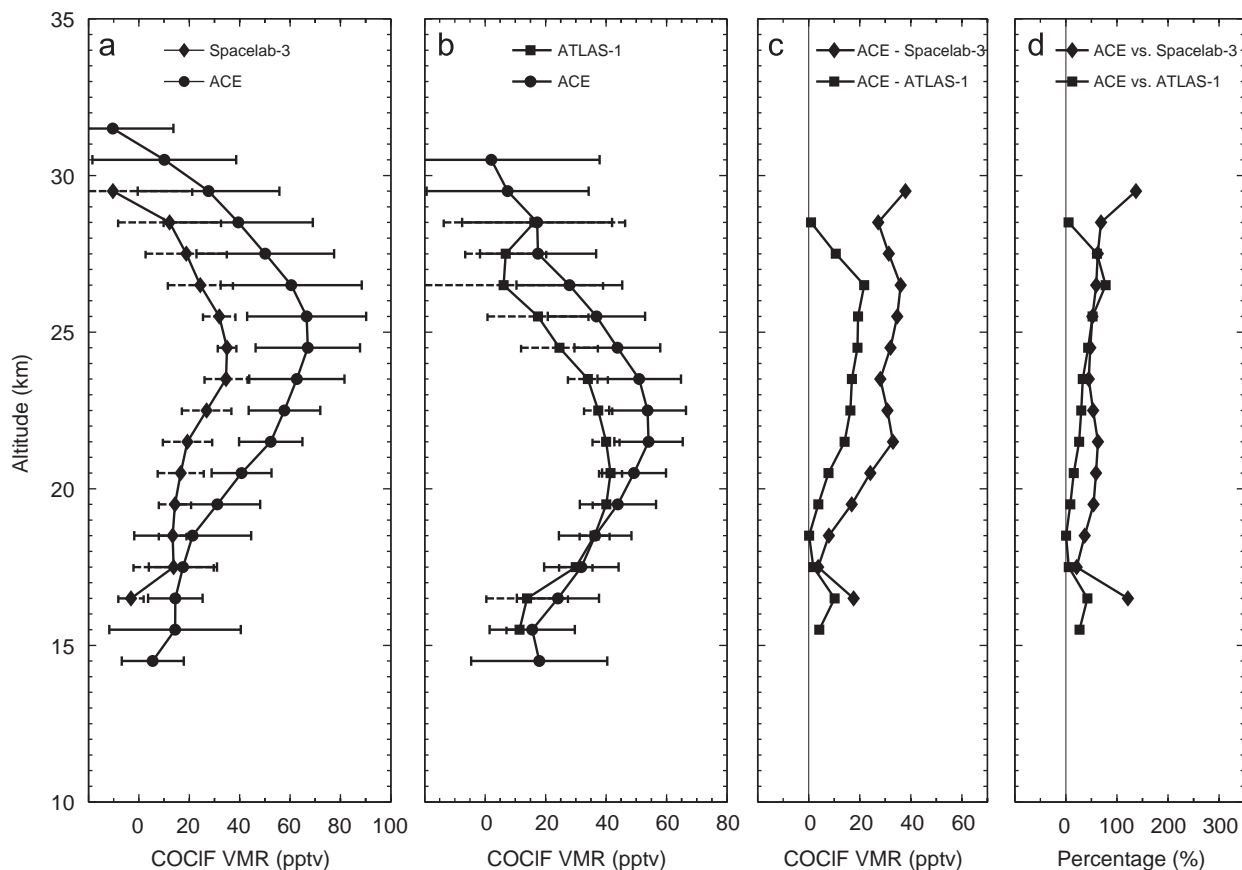


Fig. 8. Comparison of averaged COCIF VMRs as function of altitude for (a) average of 105 ACE occultations (25–30°N) vs. average of 3 Spacelab-3 occultations, (b) Average of 292 ACE occultation (35–45°S) with average of 5 ATLAS-1 occultations, (c) the differences of averaged COCIF VMR profiles between ACE measurements and the Spacelab-3, ATLAS-1 observations, respectively, (d) the percentage differences of averaged COCIF VMR profiles between ACE measurements and Spacelab-3, ATLAS-1 observations. Error bars are the standard deviation of averaged COCIF VMR profiles and represent a measure of the scatter in the data. The location, date and time of Spacelab-3 and ATLAS-1 are listed in Table 2.

such that a disproportionate number of measurements are from the lower portion of the bin, the average spectrum would not be representative of the altitude at the center of the bin, which would introduce an altitude offset in the retrieved COCIF profile.

COCIF VMRs from ACE-FTS are higher than the observations from the ATMOS measurements on Spacelab-3 and ATLAS-1. It is shown in Fig. 8 that the atmospheric COCIF levels during the period February 2004–April 2007 significantly higher than those measured by ATMOS at the corresponding latitudes in April 1985 and March 1992. The differences between the ACE-FTS and ATMOS COCIF VMRs likely arise from changes in the concentration of CFC-11, the source species of COCIF. The VMR levels of CFC-11 measured by ACE-FTS in the lower stratosphere at about 15–20 km is about twice as high as those observed on Spacelab-3 using the ATMOS instrument (not shown).

6. Summary and conclusions

The first study of the global distribution of atmospheric COCIF has been performed using measurements from the ACE satellite mission. A total of 8368 profiles from the period February 2004–April 2007 were used, after filtering out occultations that were inside or on the edge of the polar vortex. Weak seasonal variation was observed in the data. A major source region for atmospheric COCIF appears in the stratosphere over the tropics (around 27 km), where the highest VMRs (60–100 pptv) are observed, likely related to higher levels of the parent molecule (CCl_3F) in this region. A layer of enhanced COCIF exists in the low- to mid-stratosphere, a combination of in situ production and transport from the tropics through the Brewer-Dobson circulation. COCIF VMRs become negligible in the mid- to upper-stratosphere, due to loss from UV photolysis and reaction with $\text{O}(^1\text{D})$. COCIF VMRs in the troposphere are very small as a result of minimal production and removal by washout. A slight hemispheric asymmetry in COCIF arises from the hemispheric asymmetry in the parent molecule CCl_3F .

Comparisons of the ACE-FTS COCIF retrieval results with AER model predictions show good agreement. An apparent altitude offset relative to the AER model results observed in a previous study was not evident in this study, suggesting that the retrievals from averaged spectra in the previous study was likely the origin of the altitude offset. For the small altitude overlap region (13–17 km) with a set of aircraft measurements from ~20 years ago, the general behavior is in agreement with the observed COCIF VMR.

Uncertainties on the COCIF spectroscopic parameters are reported as being about 300%. Considering the excellent agreement between the retrieval results and the model calculations, this uncertainty seems overestimated. No adjustments were made to the model to improve agreement with the retrievals (or vice versa), and the agreement is remarkably good.

Acknowledgments

The Canada Space Agency (CSA) provided funding for this work. Research at AER was supported by National Aeronautics and Space Administration (NASA) Atmospheric Chemistry Modeling and Analysis Program (ACMAP). Work at NASA Langley Research Center was also supported by the ACPMAP. Work at the Jet Propulsion Laboratory, California Institute of Technology was done under contract with the National Aeronautics and Space Administration. Work at York was supported by the UK Natural Environment Research Council (NERC).

References

- [1] Zander R, Gunson MR, Farmer CB, Rinsland CP, Irion FW, Mahieu E. The 1985 chlorine and fluorine inventories in the stratosphere based on ATMOS observations at 30° North latitude. *J Atmos Chem* 1992;15:171–86.
- [2] Zander R, Mahieu E, Gunson MR, Abrams MC, Chang AY, Abbas M, et al. The 1994 northern midlatitude budget of stratospheric chlorine derived from ATMOS/ATLAS-3 observations. *Geophys Res Lett* 1996;23(17):2357–60.
- [3] Sen B, Toon GC, Blavier J-F, Fleming EL, Jackman CH. Balloon-borne observations of midlatitude fluorine abundance. *J Geophys Res* 1996;101:9045–54.
- [4] Nassar R, Bernath PF, Boone CD, Clerbaux C, Coheur PF, Dufour G, et al. A global inventory of stratospheric chlorine in 2004. *J Geophys Res* 2006;111:D22312.
- [5] Nassar R, Bernath PF, Boone CD, McLeod SD, Rinsland CP, Skelton R, et al. A global inventory of stratospheric fluorine in 2004 based on ACE-FTS measurements. *J Geophys Res* 2006;111:D22313.
- [6] Kaye JA, Douglass AR, Jackman CH, Stolarski RS, Zander R, Rowland G. Two-dimensional model calculation of fluorine containing reservoir species in the stratosphere. *J Geophys Res* 1991;96:12865–81.
- [7] Wu F, Carr RW. Time-resolved observation of the formation of CF₂O and CFCIO in the CF₂Cl+O₂ and CFCI₂+O₂ reactions. The unimolecular elimination of Cl atoms from CF₂ClO and CFCI₂O radicals. *J Phys Chem* 1992;96:1743–8.
- [8] Sze ND. Stratospheric fluorine: a composition between theory and measurements. *Geophys Res Lett* 1978;5:781–3.
- [9] Crutzen PJ, Isakosen ISA, McAfee JR. The impact of the chlorocarbon industry on the ozone layer. *J Geophys Res* 1978;83:345–63.
- [10] Wilson SR, Schuster G, Helas G. Measurements of COFCl and COCl₂ near the tropopause. In: Bojkov RD, Fabian P, editors. *Ozone in the stratosphere. Proceedings of the quadrennial ozone symposium 1988 and tropospheric ozone workshop*; 1989. p. 302–5.
- [11] Rinsland CP, Nassar R, Boone CD, Bernath PF, Chiou L, Weisenstein DK, et al. Spectroscopic detection of COCIF in the tropical and mid-latitude lower stratosphere. *JQSRT* 2007;105:467–75.
- [12] Bernath PF, McElroy CT, Abrams MC, Boone CD, Butler M, Camy-Peyret C, et al. Atmospheric Chemistry Experiment (ACE): mission overview. *Geophys Res Lett* 2005;32:L15S01.
- [13] Boone CD, Nassar R, Walker KA, Rochon Y, McLeod SD, Rinsland CP, et al. Retrievals for the atmospheric chemistry experiment Fourier-transform spectrometer. *Appl Opt* 2005;44:7218–31.
- [14] Brown LR, Farmer CB, Rinsland CP, Toth RA. Molecular line parameters for the atmospheric trace molecule spectroscopy experiment. *Appl Opt* 1987;26:5154–82.
- [15] Brown LR, Gunson MR, Toth RA, Irion FW, Rinsland CP, Goldman A. 1995 atmospheric trace molecule spectroscopy (ATMOS) linelist. *Appl Opt* 1996;35:2828–48.
- [16] Rothman LS, Jacquemart D, Barbe A, Chris Benner D, Birk M, Brown LR, et al. The HITRAN 2004 molecular spectroscopic database. *JQSRT* 2005;96:139–204.
- [17] Manney GL, Daffer WH, Zawodny JM, Bernath PF, Hoppel KW, Walker KA, et al. Solar occultation satellite data and derived meteorological products: sampling issues and comparisons with Aura MLS. *J Geophys Res* 2007;112:D24S50.
- [18] Nassar R, Bernath PF, Boone CD, Manney GL, McLeod SD, Rinsland CP, et al. ACE-FTS measurements across the edge of the winter 2004 Arctic vortex. *Geophys Res Lett* 2005;32:L15S05.
- [19] Fu D, Boone CD, Bernath PF, Walker KA, Nassar R, Manney GL, et al. Global phosgene observations from the atmospheric chemistry experiment (ACE) mission. *Geophys Res Lett* 2007;34:L17815.
- [20] Irion FW, Gunson MR, Toon GC, Chang AY, Eldering A, Mahieu E, et al. Atmospheric trace molecule spectroscopy (ATMOS) experiment version 3 data retrievals. *Appl Opt* 2002;41(33):6968–79.
- [21] Weisenstein DK, Yue GK, Ko MKW, Sze N-D, Rodriguez JM, Scott CJ. A two-dimensional model of sulfur species and aerosols. *J Geophys Res* 1997;102:13019–35.
- [22] Weisenstein DK, Ko MKW, Dyominov IG, Pitari G, Ricciardulli L, Visconti G, et al. The effects of sulfur emissions from HSCT aircraft: a 2-D model intercomparison. *J Geophys Res* 1998;103:1527–47.
- [23] Weisenstein DK, Eluszkiewicz J, Ko MKW, Scott CJ, Jackman CH, Fleming EL, et al. Separating chemistry and transport effects in two-dimensional models. *J Geophys Res* 2004;109:D18310.
- [24] WMO (World Meteorological Organization). Scientific assessment of ozone depletion. Geneva, Switzerland; 2006.
- [25] Sander SP, Friedl RR, Golden DM, Kurylo MJ, Moortgat GK, Keller-Rudek H, et al. Chemical kinetics and photochemical data for use in atmospheric studies. JPL publication 06-02, Jet Propulsion Laboratory, Pasadena, CA, 522pp. Available at: <<http://jpldataeval.jpl.nasa.gov/download.html>>; 2006.
- [26] Harries JE, Brindley HE, Sagoo PJ, Bantges RJ. Increase in greenhouse forcing inferred from the outgoing longwave radiation spectra of the Earth in 1970 and 1997. *Nature* 2001;410:355–7 and 1124 (erratum).
- [27] Coheur PF, Clerbaux C, Colin R. Spectroscopic measurements of halocarbons and hydrohalocarbons by satellite-borne remote sensors. *J Geophys Res* 2003;108(D4):4130.
- [28] Bacmeister JT, Kuell V, Offermann D, Riese M, Elkins JW. Intercomparison of satellite and aircraft observations of ozone, CFC-11, and NOy using trajectory mapping. *J Geophys Res* 1999;104(D13):16379–90.

- [29] Hoffmann L, Spang R, Kaufman M, Riese M. Retrieval of CFC-11 and CFC-12 from Envisat MIPAS observations by means of rapid radiative transfer calculations. *Adv Space Res* 2005;36(5):915–21.
- [30] Rinsland CP, Boone CD, Nassar R, Walker KA, Bernath PF, Mahieu E, et al. Trends of HF, HCl, CCl₂F₂, CCl₃F, CHClF₂ (HCFC-22), and SF₆ in the lower stratosphere from atmospheric chemistry experiment (ACE) and atmospheric trace molecule spectroscopy (ATMOS) measurements near 30°N latitude. *Geophys Res Lett* 2005;32:L16S03.
- [31] Prinn RG, Weiss RF, Fraser PJ, Simmonds PG, Cunnold DM, Alyea FN, et al. A history of chemically and radiatively important gases in air deduced from ALE/GAGE/AGAGE. *J Geophys Res* 2000;105(D14):17751–92.
- [32] Montzka SA, Butler JH, Elkins JW, Thompson TM, Clarke AD, Lock LT. Present and future trends in the atmospheric burden of ozone-depleting halogens. *Nature* 1999;398:690–4.
- [33] Thompson TM, Butler JH, Daube BC, Dutton GS, Elkins JW, Hall BD, et al, editors. Halocarbons and other atmospheric trace species. In: Schnell R, Buggle A-M, Rosson R, editors. Section 5 in climate, editor monitoring and diagnostics laboratory, Summary Report No. 27, 2002–2003, NOAA/Climate Monitoring and Diagnostics Laboratory, Boulder, Colo; 2004. p. 115–35.
- [34] Blake DR, Chen TY, Smith Jr TW, Wang CJL, Wingenter OW, Blake NJ, et al. Three-dimensional distribution of nonmethane hydrocarbons and halocarbons over the northwestern Pacific during the 1991 Pacific Exploratory Mission (PEM-West A). *J Geophys Res* 1996;101(D1):1763–78.
- [35] Blake NJ, Blake DR, Simpson IJ, Lopez JP, Johnston NAC, Swanson AL, et al. Large-scale latitudinal and vertical distributions of NMHCs and selected halocarbons in the troposphere over the Pacific Ocean during the March–April 1999 Pacific Exploratory Mission (PEM-Tropics B). *J Geophys Res* 2001;106(D23):32627–44.